Condensed Matter Physics 2007, Vol. 10, No 2(50), pp. 165–172

CONDENSED MATTER PHYSICS

Ground-state diagrams for lattice-gas models of catalytic CO oxidation

I.M.Mryglod, I.S.Bzovska

Institute for Condensed Matter Physics of the National Academy of Sciences of Ukraine, 1 Svientsitskii Str., 79011 Lviv, Ukraine

Received April 12, 2007, in final form May 17, 2007

Based on simple lattice models of catalytic carbon dioxide synthesis from oxygen and carbon monoxide, phase diagrams are investigated at temperature $T = 0$ by incorporating the nearest-neighbor interactions on a catalyst surface. The main types of ground-state phase diagrams of two lattice models are classified describing the cases of clean surface and surface containing impurities. Nonuniform phases are obtained and the conditions of their existence dependent on the interaction parameters are established.

Key words: *lattice-gas model, catalysis, oxidation, ground state, carbon monoxide, oxygen*

PACS: *05.50.+q, 05.70.Fh, 82.20.Db, 82.65.+r*

1. Introduction

CO_2 formation through catalytic oxidation of CO is one of the prototypical surface reactions that has been extensively studied in recent years [1–10]. Much of the today's insight into heterogeneous catalysis arises from this model system. A promising concept of this reaction was introduced by Ziff et al. [11] as a computer simulation model which is known to be the ZGB model.

As an attempt of a more realistic description of CO oxidation we consider a variation of the ZGB model by incorporating O–O, CO–CO and CO–O interactions. Furthermore, one of the models investigated is the model of the reaction on the surface containing impurities since the impurities decrease the number of available adsorption sites on the surface and can drastically effect the behavior of the system. This paper is devoted to the analysis of the ground state of two models describing the cases of a clean surface and the surface containing impurities. The surface of a catalyst is simulated as a square lattice.

It is known experimentally that O atoms form ordered islands at low temperatures and higher oxygen partial pressures and CO molecules start burning oxygen in the perimeters of O–islands [12,13]. This investigation is important to approve of the models in comparison with experiments which allows us to reveal the surface structures at temperature $T = 0$. It is also interesting to find the conditions of the existence of CO–O region where the reaction of catalytic CO oxidation takes place.

2. Model I

Let us consider a two-dimensional lattice model with the Hamiltonian

$$H^* = -\mu_1 \sum_i n_i^1 - \mu_2 \sum_i n_i^2 + w_1^* \sum_{\langle ij \rangle} n_i^1 n_j^1 + w_2^* \sum_{\langle ij \rangle} n_i^2 n_j^2 + \varepsilon_{12}^* \sum_{\langle ij \rangle} n_i^1 n_j^2 \,, \tag{1}$$

where μ_1 and μ_2 denote the chemical potentials of CO and O respectively, and w_1, w_2, ε_{12} are the interaction energies between nearest-neighbor CO–CO, O–O and CO–O, respectively. The following notations for two types of adsorbate occupancies of ith surface site are: n_i^1 for an adsorbed CO molecule and n_i^2 for adsorbed oxygen where $n_i^l = [0,1]$ and l=1, 2. The condition $n_i^1 + n_i^2 \leqslant 1$ precludes the adsorbed particles from occupation of the same adsorption site. $\sum_{\langle ij \rangle}$ means the sum over the nearest-neighbor pairs.

The model was proposed by N. Pavlenko et al. in [8] where they have taken into account the short-range correlations between coadsorbates to analytically describe the alkali-modified CO oxidation reaction on a transition metal surface. In the present work we shall consider the model at zero temperature to reveal the states that are realized on a surface at low temperatures.

In our study we shall follow the method proposed in [14]. The idea of the method is as follows. If the Hamiltonian of the system can be rewritten in the form of a sum over the nearest-neighbor bonds on a lattice, then the region on the phase diagram which corresponds to this particular bond is determined from the condition of the minimum of energy of this bond. It should be noted that this method allows us to construct the ground-state diagrams only for the so-called diatomic or unfrustrated lattices. We shall consider a two-dimensional square lattice with the same number z of bonds around each site. So, let us rewrite Hamiltonian (1) replacing the sum over the sites by the sum over the bonds. Instead of the Hamiltonian H^* we shall consider the Hamiltonian $H = zH^*$:

$$H = -\mu_1 \sum_{\langle ij \rangle} (n_i^1 + n_j^1) - \mu_2 \sum_{\langle ij \rangle} (n_i^2 + n_j^2) + w_1 \sum_{\langle ij \rangle} n_i^1 n_j^1 + w_2 \sum_{\langle ij \rangle} n_i^2 n_j^2 + \varepsilon_{12} \sum_{\langle ij \rangle} n_i^1 n_j^2 \,, \qquad (2)$$

where for a hypercubic d-dimensional lattice $z = 2d$, so that for d=2 one has $w_1 = 4w_1^*$, $w_2 = 4w_2^*$ and $\varepsilon_{12} = 4\varepsilon_{12}^*$. Obviously, the ground-state diagrams are the same for both Hamiltonians (1) and (2).

Let us consider all possible states on this separate bond and note their energies. They are shown in table 1, where * denotes an empty site on a surface.

Table 1. Two-site blocks and their energies.

Block	Energy
–	0
*–CO	$-\mu_1$
*–O	$-\mu_2$
CO–CO	$w_1 - 2\mu_1$
O–O	$w_2 - 2\mu_2$
CO–O	$\varepsilon_{12} - \mu_1 - \mu_2$

We shall construct the ground-state diagrams in the (μ_1, μ_2) plane. Each region on this plane corresponding to a separate two-site block is determined by a system of inequalities obtained from the condition of the minimum of the block energy. The uniform regions *–*, CO–CO and O–O exist always, the region CO–O, where the reaction of catalytic CO oxidation takes place exists at the condition $\varepsilon_{12} < (w_1 + w_2)/2$. The nonuniform regions *–CO, *–O exist at the conditions $w_1 > 0$, $w_2 > 0$, respectively. The increase of the interaction parameters w_1 and w_2 leads to a corresponding extension of the regions *–CO, *–O. And vice versa, the region CO–O is extended with a decrease of the parameter ε_{12}. If $\varepsilon_{12} > (w_1 + w_2)/2$, $w_1 < 0$, $w_2 < 0$ there are no nonuniform phases at all.

The ground-state diagrams of the model are shown in figures 1 and 2. The coordinates of intersection points on the diagrams can be calculated analytically. As an example, we represent them for the poorest diagram (figure 1a) and for one of the richest (figure 2a) diagrams. For the first diagram, the coordinates of the intersection point are $(w_1/2, w_2/2)$. The second diagram where all the nonuniform regions exist has four intersection points with the following coordinates: point I – (ε_{12}, w_2), II – $(\varepsilon_{12}, \varepsilon_{12})$, III – (w_1, ε_{12}) and IV – (0, 0). The coordinates of intersection points for other diagrams can also be found easily.

The diagrams are symmetric with respect to the bisectrix of the angle $\mu_2 O \mu_1$. Actually, replacing the axes μ_1 and μ_2 as well as the notations CO and O we shall obtain the same diagrams. For example, these are figures 1(b) and 1(c), 1(e) and 1(f), and so on.

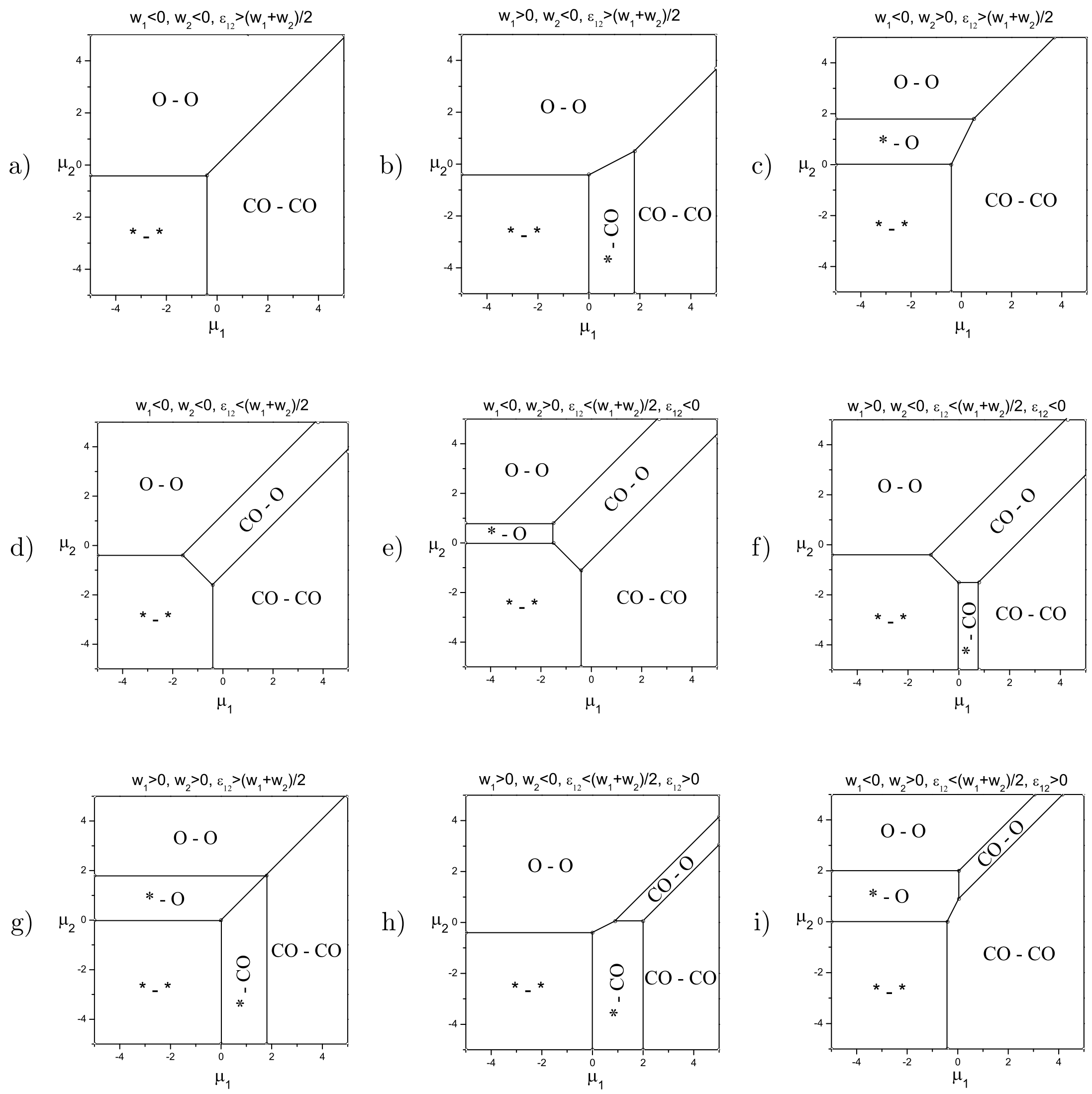

Figure 1. Main topologies of ground-state diagrams for the model I. The parameters are given in kcal/mol. (a) $w_1 = -0.8$, $w_2 = -0.8$, $\varepsilon_{12} = 1.5$; (b) $w_1 = 1.8$, $w_2 = -0.8$, $\varepsilon_{12} = 1.5$; (c) $w_1 = -0.8$, $w_2 = 1.8$, $\varepsilon_{12} = 1.5$; (d) $w_1 = -0.8$, $w_2 = -0.8$, $\varepsilon_{12} = -2$; (e) $w_1 = -0.8$, $w_2 = 0.8$, $\varepsilon_{12} = -1.5$; (f) $w_1 = 0.8$, $w_2 = -0.8$, $\varepsilon_{12} = -1.5$; (g) $w_1 = 1.8$, $w_2 = 1.8$, $\varepsilon_{12} = 2.5$; (h) $w_1 = 2$, $w_2 = -0.8$, $\varepsilon_{12} = 0.05$; (i) $w_1 = -0.8$, $w_2 = 2$, $\varepsilon_{12} = 0.05$.

As one can see, twelve topologically nonequivalent diagrams are obtained: eight types of diagrams for $\varepsilon_{12} < (w_1 + w_2)/2$ where the region CO–O exists (figure 1(d, e, f, h, i) and figure 2) and four diagrams for $\varepsilon_{12} > (w_1 + w_2)/2$ without this region (figure 1(a, b, c, g)). We note that model (1) is isomorphous to a spin–1 Ising model.

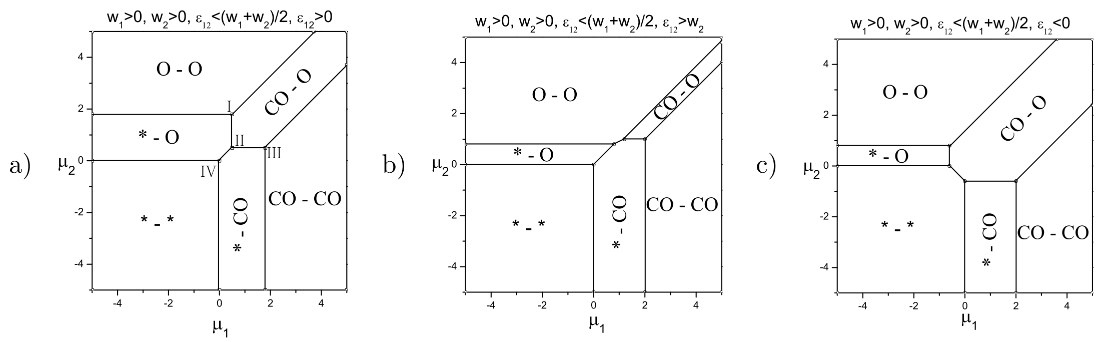

Figure 2. Topologies of ground-state diagrams for the model I in the case $w_1 > 0$, $w_2 > 0$, $\varepsilon_{12} < (w_1 + w_2)/2$. The parameters are given in kcal/mol. (a) $w_1 = 1.8$, $w_2 = 1.8$, $\varepsilon_{12} = 0.5$; (b) $w_1 = 2$, $w_2 = 0.8$, $\varepsilon_{12} = -0.6$; (c) $w_1 = 2$, $w_2 = 0.8$, $\varepsilon_{12} = 1$.

3. Model II

Now let us consider a model of the reaction of catalytic CO oxidation by incorporating the effect of passive impurities on a surface. In the case when impurities can be considered as equilibrium ones, the Hamiltonian of the system is

$$\begin{aligned} H^* &= -\mu_1 \sum_i n_i^1 - \mu_2 \sum_i n_i^2 + w_1^* \sum_{\langle ij \rangle} n_i^1 n_j^1 + w_2^* \sum_{\langle ij \rangle} n_i^2 n_j^2 + \varepsilon_{12}^* \sum_{\langle ij \rangle} n_i^1 n_j^2 \\ &\quad + \varepsilon_{13}^* \sum_{\langle ij \rangle} n_i^1 n_j^3 + \varepsilon_{23}^* \sum_{\langle ij \rangle} n_i^2 n_j^3 \,, \end{aligned} \tag{3}$$

where n_i^3 denotes ith surface site occupied by an impurity, ε_{13} and ε_{23} are the interaction energies between the nearest-neighbor CO – impurity and O – impurity, respectively. We suppose that the average coverage of impurities $\langle n^3 \rangle \ll 1$ that is why the interactions between the nearest-neighbor impurity – impurity can be neglected. It should be noted that the obvious separation of impurities in Hamiltonian (3) ($n^3 \to c$, where c denotes the impurity concentration) leads model (3) to model (1) with the renormalized parameters, namely $\mu_1 \to \mu_1 - \varepsilon_{13}^* zc$ and $\mu_2 \to \mu_2 - \varepsilon_{23}^* zc$. At temperature $T = 0$, the entropy makes zero contribution to the thermodynamic potential and there are only contributions from the average energy and the number of particles. Consequently, in this approximation a shift of the phases along the axes $0\mu_1$, $0\mu_2$ can be observed in the phase diagrams obtained for model (1).

We rewrite Hamiltonian (3) replacing the sum over the sites by the sum over the bonds. In an analogy to the previous model, instead of the Hamiltonian H^* we consider the Hamiltonian $H = zH^*$ that has the following form

$$\begin{aligned} H &= -\mu_1 \sum_{\langle ij \rangle} (n_i^1 + n_j^1) - \mu_2 \sum_{\langle ij \rangle} (n_i^2 + n_j^2) + w_1 \sum_{\langle ij \rangle} n_i^1 n_j^1 + w_2 \sum_{\langle ij \rangle} n_i^2 n_j^2 + \varepsilon_{12} \sum_{\langle ij \rangle} n_i^1 n_j^2 \\ &\quad + \varepsilon_{13} \sum_{\langle ij \rangle} n_i^1 n_j^3 + \varepsilon_{23} \sum_{\langle ij \rangle} n_i^2 n_j^3 \,, \end{aligned} \tag{4}$$

where the notations $w_1 = 4w_1^*$, $w_2 = 4w_2^*$, $\varepsilon_{12} = 4\varepsilon_{12}^*$, $\varepsilon_{13} = 4\varepsilon_{13}^*$ and $\varepsilon_{23} = 4\varepsilon_{23}^*$ are introduced.

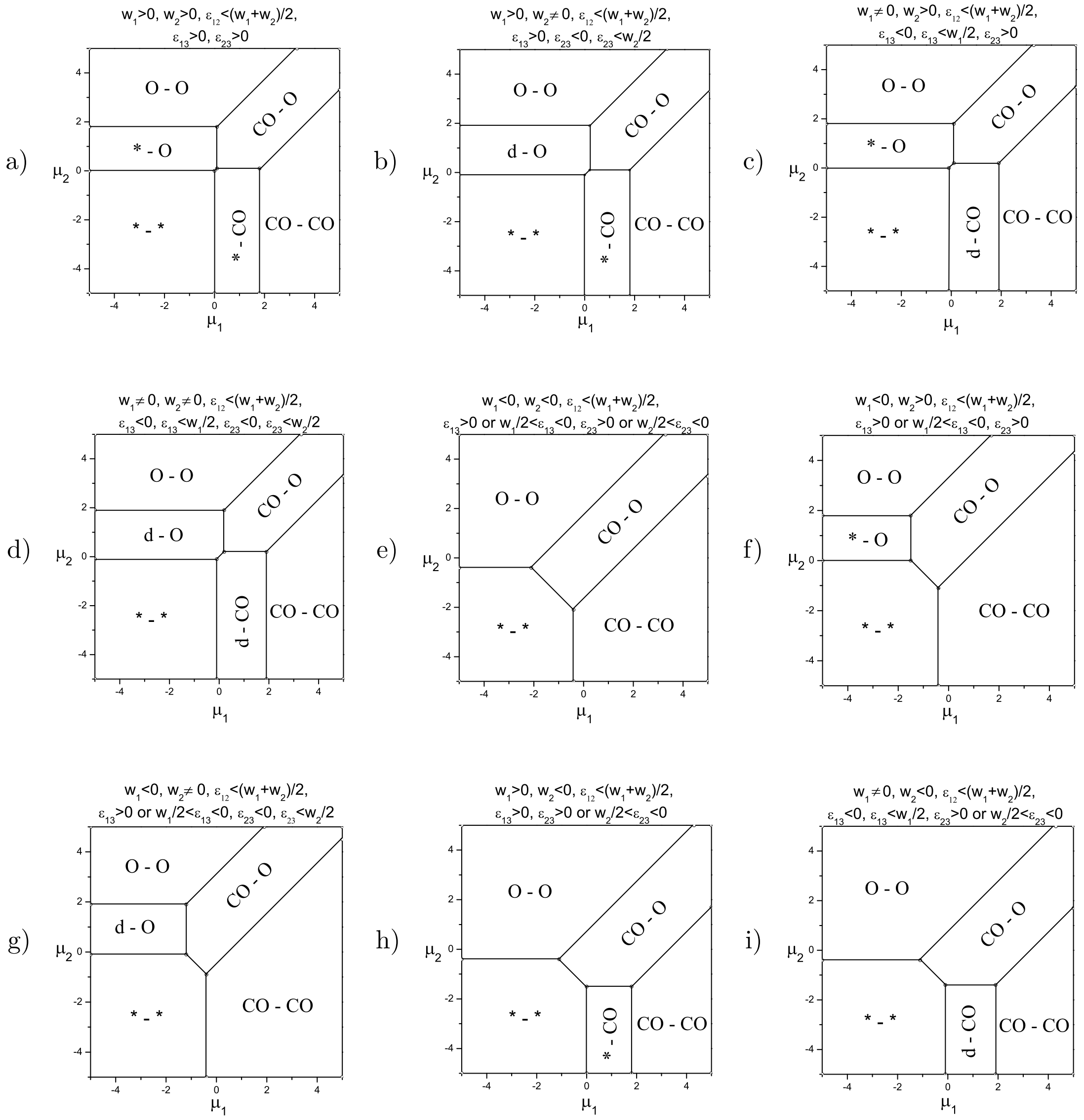

Figure 3. Main topologies of ground-state diagrams for the model II that takes into account passive impurities in the case $\varepsilon_{12} < \frac{1}{2}(w_1+w_2)$. The parameters are given in kcal/mol. (a) $w_1 = 1.8$, $w_2 = 1.8$, $\varepsilon_{12} = 0.1$, $\varepsilon_{13} = 1.3$, $\varepsilon_{23} = 1.3$; (b) $w_1 = 1.8$, $w_2 = 1.8$, $\varepsilon_{12} = 0.1$, $\varepsilon_{13} = 0.1$, $\varepsilon_{23} = -0.1$; (c) $w_1 = 1.8$, $w_2 = 1.8$, $\varepsilon_{12} = 0.1$, $\varepsilon_{13} = -0.1$, $\varepsilon_{23} = 0.1$; (d) $w_1 = 1.8$, $w_2 = 1.8$, $\varepsilon_{12} = 0.1$, $\varepsilon_{13} = -0.1$, $\varepsilon_{23} = -0.1$; (e) $w_1 = -0.8$, $w_2 = -0.8$, $\varepsilon_{12} = -2.5$, $\varepsilon_{13} = 1.8$, $\varepsilon_{23} = 1.8$; (f) $w_1 = -0.8$, $w_2 = 1.8$, $\varepsilon_{12} = -1.5$, $\varepsilon_{13} = 1.8$, $\varepsilon_{23} = 1.8$; (g) $w_1 = -0.8$, $w_2 = 1.8$, $\varepsilon_{12} = -1.3$, $\varepsilon_{13} = 0.1$, $\varepsilon_{23} = -0.1$; (h) $w_1 = 1.8$, $w_2 = -0.8$, $\varepsilon_{12} = -1.5$, $\varepsilon_{13} = 1.8$, $\varepsilon_{23} = 1.8$; (i) $w_1 = 1.8$, $w_2 = -0.8$, $\varepsilon_{12} = -1.5$, $\varepsilon_{13} = -0.1$, $\varepsilon_{23} = 0.1$.

All the possible bonds and the corresponding energies are given in table 2. Let us construct the ground-state diagrams in the (μ_1, μ_2) plane. The uniform regions *–*, CO–CO and O–O, as in the previous case, exist always, the region CO–O where the reaction of catalytic CO oxidation takes place exists at the same condition $\varepsilon_{12} < (w_1 + w_2)/2$. The region *–CO exists at the conditions $w_1 > 0$ and $\varepsilon_{13} > 0$. Similarly the region *–O exists at the conditions $w_2 > 0$ and $\varepsilon_{23} > 0$. The nonuniform region d–CO exists at the conditions $\varepsilon_{13} < 0$ and $\varepsilon_{13} < w_1/2$, d–O – at the conditions $\varepsilon_{23} < 0$ and $\varepsilon_{23} < w_2/2$. The regions *–CO and d–CO as well as the regions *–O and d–O cannot

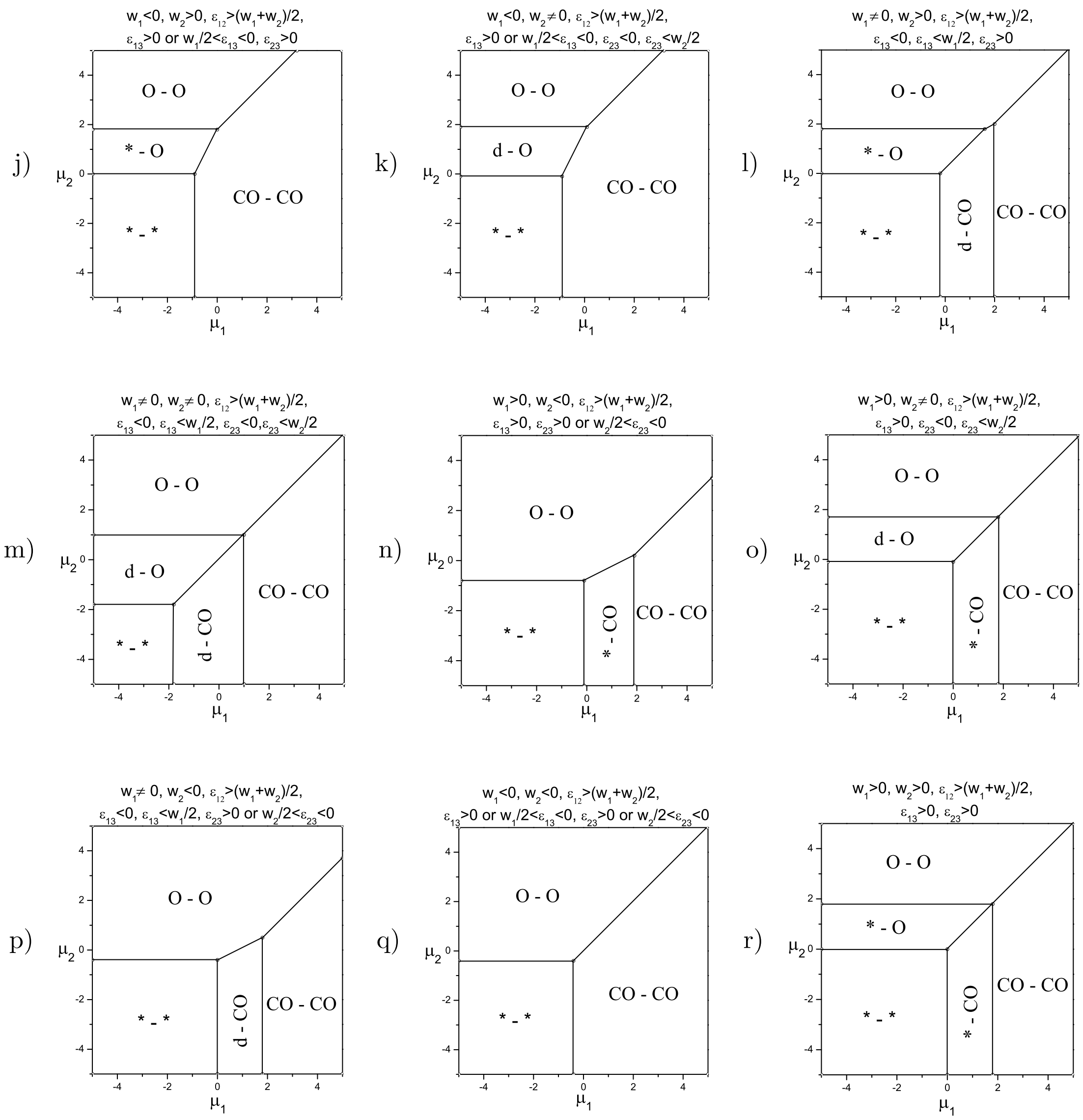

Figure 4. Main topologies of ground-state diagrams for the model II in the case $\varepsilon_{12} > \frac{1}{2}(w_1{+}w_2)$. The parameters are given in kcal/mol. (j) $w_1 = -1.8$, $w_2 = 1.8$, $\varepsilon_{12} = 0.5$, $\varepsilon_{13} = 0.8$, $\varepsilon_{23} = 0.8$; (k) $w_1 = -1.8$, $w_2 = 1.8$, $\varepsilon_{12} = 0.5$, $\varepsilon_{13} = 0.8$, $\varepsilon_{23} = -0.1$; (l) $w_1 = 1.8$, $w_2 = 1.8$, $\varepsilon_{12} = 2.5$, $\varepsilon_{13} = -0.2$, $\varepsilon_{23} = 0.2$; (m) $w_1 = -0.8$, $w_2 = -0.8$, $\varepsilon_{12} = 0.5$, $\varepsilon_{13} = -1.8$, $\varepsilon_{23} = -1.8$; (n) $w_1 = 1.8$, $w_2 = -0.8$, $\varepsilon_{12} = 1.5$, $\varepsilon_{13} = 1.8$, $\varepsilon_{23} = 1.8$; (o) $w_1 = 1.8$, $w_2 = 1.6$, $\varepsilon_{12} = 2.5$, $\varepsilon_{13} = 0.1$, $\varepsilon_{23} = -0.1$; (p) $w_1 = 1.8$, $w_2 = -1.6$, $\varepsilon_{12} = 1.5$, $\varepsilon_{13} = -0.1$, $\varepsilon_{23} = 0.1$; (q) $w_1 = -0.8$, $w_2 = -0.8$, $\varepsilon_{12} = 2.5$, $\varepsilon_{13} = 1.8$, $\varepsilon_{23} = 1.8$; (r) $w_1 = 1.8$, $w_2 = 1.8$, $\varepsilon_{12} = 2.5$, $\varepsilon_{13} = 0.1$, $\varepsilon_{23} = 0.1$.

exist simultaneously. In the case $\varepsilon_{12} > (w_1 + w_2)/2$, $w_1 < 0$, $w_2 < 0$, $\varepsilon_{13} > 0$ and $\varepsilon_{23} > 0$ none of the nonuniform regions exists.

The ground-state diagrams of the model are shown in figures 3 and 4. There are eighteen topologically nonequivalent diagrams in this model: nine for $\varepsilon_{12} < (w_1 + w_2)/2$ when the region CO–O exists (figure 3) and nine for $\varepsilon_{12} > (w_1 + w_2)/2$ without this region (figure 4). This model is isomorphous to a spin–3/2 Ising model.

Table 2. Two-site blocks and their energies.

Block	Energy
_	0
*–CO	$-\mu_1$
*–O	$-\mu_2$
d–CO	$\varepsilon_{13} - \mu_1$
d–O	$\varepsilon_{23} - \mu_2$
CO–CO	$w_1 - 2\mu_1$
O–O	$w_2 - 2\mu_2$
CO–O	$\varepsilon_{12} - \mu_1 - \mu_2$

4. Conclusions

Thus, using the method, developed in [14], we have constructed the ground-state diagrams for two lattice models of the catalytic reaction of carbon dioxide synthesis by incorporating the nearest-neighbor interactions between coadsorbates. We have investigated the model I of the reaction taking place on a surface without any impurities as well as the model II that describes the reaction on a surface containing passive impurities. These models have been analysed for a two-dimensional square lattice. For both models we have found the conditions of the existence of nonuniform phases depending on the interaction parameters. The nonuniform region CO–O, where the reaction of catalytic CO oxidation takes place, exists at the same condition $\varepsilon_{12} < (w_1 + w_2)/2$ for both models. The width of this region increases when the interaction parameter ε_{12} decreases. At the model parameters used in [8] a topology of the ground-state phase diagram is similar to that shown in figure 1(e). It is worth noting that the separation of impurities in the Hamiltonian of the model II leads to the model I with the renormalized parameters and to a corresponding shift of phases along the axes $0\mu_1$, $0\mu_2$ in the phase diagrams. The direction of such a shift depends on the sign of interaction parameters ε_{13} and ε_{23}, describing the coupling of CO and O with impurities, respectively. The models considered are equivalent to spin–1 and spin–3/2 Ising models.

Acknowledgements

The authors thank Yu.I. Dublenych for his valuable comments and discussions.

References

1. Baxter R.J., Hu P., J. Chem. Phys., 2002, **116**, 4379.
2. Han S.-J., Lee C.-W., Yoon H., Kang H., J. Chem. Phys., 2002, **116**, 2684.
3. Grandi B.C.S., Figueiredo W., Phys. Rev. E, 2002, **65**, 036135.
4. Cisternas Y., Holmes Ph., Kevrekidis I.G., Li X., J. Chem. Phys., 2003, **118**, 3312.
5. Peskov N.V., Slinko M.M., Jaeger N.I., J. Chem. Phys., 2002, **116**, 2098.
6. Chavez F., Vicente L., Perera A., J. Chem. Phys., 2000, **113**, 10353.
7. Nekhamkina O., Digilov R., Sheintuch M., J. Chem. Phys., 2003, **119**, 2322.
8. Pavlenko N., Kostrobij P.P., Suchorski Yu., Imbihl R., Surf. Sci., 2001, **489**, 29.
9. Khan K.M., Albano E.V., Chem. Phys., 2002, **276**, 129.
10. Kostrobii P.P., Tokarchuk M.V., Alekseyev V.I., Phys. and Chem. of Solid State, 2006, **7**, No. 1, 25 (in Ukrainian).
11. Ziff R.M., Gulari E., Barshad Y., Phys. Rev. Lett., 1986, **56**, 2553.
12. Gland J.L., Fisher G.B., Kollin E.B., J. Catal., 1982, **77**, 263.
13. Verheij L.K., Hugenschmidt M.B., Surf. Sci., 1995, **324**, 185.
14. Dublenych Yu.I., Phys. Rev. B, 2005, **71**, 012411.

Діаграми основного стану для ґраткових моделей каталітичного окислення CO

І.М.Мриглод, І.С.Бзовська

Інститут фізики конденсованих систем НАН України, вул. Свєнціцького, 1, 79011 Львів, Україна

Received April 12, 2007, in final form May 17, 2007

В рамках простих ґраткових моделей каталітичного синтезу вуглекислого газу з кисню та чадного газу досліджуються фазові діаграми при температурі $T = 0$ із врахуванням взаємодій на поверхні між найближчими сусідами. Прокласифіковано основні типи фазових діаграм основного стану для моделей без домішок та у випадку присутності домішок. Знайдено умови існування неоднорідних областей залежно від значень параметрів взаємодії.

Ключові слова: *модель ґраткового газу, каталіз, окислення, основний стан, монооксид вуглецю, кисень*

PACS: *05.50.+q, 05.70.Fh, 82.20.Db, 82.65.+r*